



Birchall, P. M., Allen, E. J., Stace, T. M., O'Brien, J. L., Matthews, J. C. F., & Cable, H. (2020). Quantum Optical Metrology of Correlated Phase and Loss. *Physical Review Letters*, 124(140501), 140501. <https://doi.org/10.1103/PhysRevLett.124.140501>

Peer reviewed version

Link to published version (if available):
[10.1103/PhysRevLett.124.140501](https://doi.org/10.1103/PhysRevLett.124.140501)

[Link to publication record in Explore Bristol Research](#)
PDF-document

University of Bristol - Explore Bristol Research

General rights

This document is made available in accordance with publisher policies. Please cite only the published version using the reference above. Full terms of use are available:
<http://www.bristol.ac.uk/red/research-policy/pure/user-guides/ebr-terms/>

Quantum Optical Metrology of Correlated Phase and Loss

Patrick M. Birchall,¹ Euan J. Allen,^{1,2,*} Thomas M. Stace,³ Jeremy L. O'Brien,¹ Jonathan C. F. Matthews,¹ and Hugo Cable¹

¹Quantum Engineering Technology Labs, H. H. Wills Physics Laboratory and Department of Electrical & Electronic Engineering, University of Bristol, BS8 1FD, United Kingdom.

²Quantum Engineering Centre for Doctoral Training, H. H. Wills Physics Laboratory and Department of Electrical & Electronic Engineering, University of Bristol, Tyndall Avenue, BS8 1FD, United Kingdom.

³ARC Centre of Excellence for Engineered Quantum Systems, School of Mathematics and Physics, University of Queensland, Saint Lucia, Queensland 4072, Australia.

(Dated: March 11, 2020)

Optical absorption measurements characterize a wide variety of systems from atomic gases to *in-vivo* diagnostics of living organisms. Here we study the potential of non-classical techniques to reduce statistical noise below the shot-noise limit in absorption measurements with concomitant phase shifts imparted by a sample. We consider both cases where there is a known relationship between absorption and a phase shift, and where this relationship is unknown. For each case we derive the fundamental limit and provide a practical strategy to reduce statistical noise. Furthermore, we find an intuitive correspondence between measurements of absorption and of lossy phase shifts, which both show the same analytical form for precision enhancement for bright states. Our results demonstrate that non-classical techniques can aid real-world tasks with present-day laboratory techniques.

The precision of optically measuring an object is limited by fundamental fluctuations in the optical field due to the quantum nature of light [1]. When using laser light as an optical probe, the limit of this statistical noise is the shot-noise limit which can be reduced by increasing probe intensity or enhancing interaction with the sample. However, some systems are incompatible with increased intensities, for example if light causes undesired technical effects [2, 3] or the sample to deform [4, 5]. If high-intensity light cannot be used then shot-noise will limit the achievable precision [2, 3, 6].

Whilst of a fundamental origin, shot-noise is not the ultimate quantum limit — non-classical probes can be used to exceed the shot-noise limit [7]. Many previous theoretical and experimental studies have investigated potential benefits of using non-classical states for phase estimation in the presence of loss [8–14], and for loss estimation [5, 10, 15–21]. In addition, a number of studies have investigated quantum bounds for multiparameter estimation including unitary [22–24] and non-unitary [25–27] channels.

At a fundamental level, changes in absorption over a narrow spectral range must be accompanied by changes in refractive index (and hence phase shifts), governed by the Kramers-Kronig relations [28]. It is therefore important to consider how the estimation capabilities of any strategy are affected by correlation between these two variables. Here we address this and seek a unified understanding of optimal quantum strategies for measuring a single parameter which drives both absorption and phase of a single optical mode. We consider estimating an unknown parameter χ , which governs both phase $\theta(\chi) \in [0, 2\pi)$ and loss $1 - \eta(\chi) \in [0, 1]$ imparted by a channel Λ_χ which we call correlated phase and loss estimation (CPLE). Formally, Λ_χ is defined by its action on a basis of coherent states $|\alpha\rangle \xrightarrow{\Lambda_\chi} |\sqrt{\eta}e^{i\theta}\alpha\rangle$. Lossy-phase estimation ($\partial_\chi\eta = 0$ where $\partial_\bullet \equiv \frac{\partial}{\partial \bullet}$) and loss estimation ($\partial_\chi\theta = 0$) [16–18] are special cases of CPLE.

We first find the fundamental upper bound on the precision

achievable with CPLE, quantified using the quantum Fisher information (QFI) per input photon. We investigate the saturability of this bound using squeezed coherent states, which can readily be generated experimentally [29]. We also consider direct absorption estimation (DAE), where $\eta(\chi)$ is to be estimated but its relationship to $\theta(\chi)$ is not known and therefore the information contained in the phase cannot be accessed. By explicitly considering large displacements, Eq.(11), we find that the quantum advantage for both DAE and CPLE have the same analytical form and dependence on the input state squeezing parameter r and total channel transmission η . We conclude by investigating multi-pass strategies for CPLE and DAE, and by investigating the advantage attainable in all cases by current experimental capabilities.

Fundamental limit for CPLE — We use the established Fisher information (FI) formalism to provide bounds on precision for estimating an unknown parameter χ encoded within a quantum state ϱ_χ :

$$\frac{1}{\text{Var}(\chi)} \stackrel{1}{\leq} F_M^\chi(\varrho_\chi) \stackrel{2}{\leq} \mathcal{F}^\chi(\varrho_\chi).$$

Inequality 1 is the Crámer–Rao bound (CRB) [30] and relates the variance of unbiased estimates $\text{Var}(\chi)$ to the FI $F_M^\chi(\varrho_\chi) = \sum_i p(i|\chi) [\partial_\chi \log p(i|\chi)]^2$. The FI is a function of the probabilities $p(i|\chi) = \text{tr}(m_i \varrho_\chi)$, given by the measurement of ϱ_χ , with a positive-operator valued measure (POVM) $M = \{m_i\}$ and $\sum_i m_i = \mathbb{1}$. Inequality 2 is the quantum CRB [31] which relates $F_M^\chi(\varrho_\chi)$ to its maximum value \mathcal{F}^χ (the QFI) which is found by optimizing over all POVMs [32]. \mathcal{F} serves as a measurement basis independent evaluation of the information that ϱ_χ contains on χ . When χ is encoded onto a pure probe state by unitary $\mathcal{U}_\chi|\psi\rangle = |\psi^\chi\rangle$ the QFI becomes $4(\|\partial_\chi\psi^\chi\|^2 - |\langle\psi^\chi|\partial_\chi\psi^\chi\rangle|^2)$ where $|\partial_\bullet\psi\rangle \equiv \partial_\bullet|\psi\rangle$ and $\|\bullet\|$ is the 2-norm.

Loss enacts a non-unitary evolution. Ref. [13] showed that

for such a non-unitary map Λ_χ acting on a pure state $|\psi\rangle$,

$$\mathcal{F}[\Lambda_\chi(|\psi\rangle)] = \min_{\mathcal{U}_\chi} (\mathcal{F}[\mathcal{U}_\chi|\psi\rangle_S|0\rangle_E]), \quad (1)$$

where \mathcal{U}_χ is a unitary dilation of the channel, acting on a larger Hilbert space containing system mode S and environment mode E , and satisfying $\Lambda_\chi(\bullet) = \text{tr}_E [\mathcal{U}_\chi(\bullet_S \otimes |0\rangle\langle 0|_E)\mathcal{U}_\chi^\dagger]$. For lossy-phase estimation \mathcal{U}_χ can be chosen such that $\mathcal{F}[\mathcal{U}_\chi|\psi\rangle_S|0\rangle_E]$ provides informative bounds on the achievable precision dependent only on the mean number of probe photons $\langle \hat{n} \rangle_{\text{in}} \equiv \langle \psi | \hat{n}_S | \psi \rangle$ [13].

Seeking an upper bound on the precision for CPLE we choose a unitary dilation of S , with a single free environmental parameter ς which dictates the phase imparted onto E . This dilation takes the form $\mathcal{U}_{\chi,\varsigma} = U_2(\theta, \varsigma)U_1(\eta)$ where $U_1(\eta)$ and $U_2(\theta, \varsigma)$ enact system loss $(1-\eta)$ and phase θ of \mathcal{U} respectively. These unitaries are given by $U_1 = \exp[i\hat{H}_1\xi(\eta)]$, $\hat{H}_1 = \frac{i}{2}(\hat{a}_S^\dagger \hat{a}_E - \hat{a}_E^\dagger \hat{a}_S)$, $\xi(\eta) = \arccos(2\eta - 1)$ and $U_2 = \exp[i\hat{H}_2(\varsigma)\theta]$, $\hat{H}_2(\varsigma) = \hat{n}_S + \varsigma \hat{n}_E$. We verify that \mathcal{U}_χ is a dilation of Λ_χ in Supplementary Material A [33]. In Supplementary Material B [33] we show that for $|\Psi_{\chi,\varsigma}\rangle \equiv \mathcal{U}_{\chi,\varsigma}|\psi\rangle_S|0\rangle_E$:

$$\begin{aligned} \mathcal{F}^\chi(|\Psi_{\chi,\varsigma}\rangle) &= (\partial_\chi \theta)^2 4 \left(\|\partial_\theta \Psi_{\chi,\varsigma}\|^2 - |\langle \Psi_{\chi,\varsigma} | \partial_\theta \Psi_{\chi,\varsigma} \rangle|^2 \right) \\ &\quad + (\partial_\chi \eta)^2 4 \left(\|\partial_\eta \Psi_{\chi,\varsigma}\|^2 - |\langle \Psi_{\chi,\varsigma} | \partial_\eta \Psi_{\chi,\varsigma} \rangle|^2 \right). \end{aligned} \quad (2)$$

For any probe state, the second term in Eq. (2) is given by:

$$(\partial_\chi \eta)^2 4 \left(\|\partial_\eta \Psi_{\chi,\varsigma}\|^2 - |\langle \Psi_{\chi,\varsigma} | \partial_\eta \Psi_{\chi,\varsigma} \rangle|^2 \right) = \frac{(\partial_\chi \eta)^2 \langle \hat{n} \rangle_{\text{in}}}{\eta(1-\eta)},$$

which is independent of ς [33]. Therefore, the optimal ς is given by minimization of $\|\partial_\theta \Psi_{\chi,\varsigma}\|^2 - |\langle \Psi_{\chi,\varsigma} | \partial_\theta \Psi_{\chi,\varsigma} \rangle|^2$, in accordance with Eq. (1). This same expression was minimized in Ref. [13] and hence has the same optimal value:

$$\varsigma_{\text{opt}} = 1 - \text{Var}_{\text{in}}(\hat{n}) / [(1-\eta) \text{Var}_{\text{in}}(\hat{n}) + \eta \langle \hat{n} \rangle_{\text{in}}], \quad (3)$$

with $\text{Var}_{\text{in}}(\hat{n}) = \langle \psi | \hat{n}_S^2 | \psi \rangle - (\langle \hat{n} \rangle_{\text{in}})^2$. Therefore the limit we have found for CPLE is simply the sum of the limits on QFI for phase estimation (first term) and loss estimation (second term) [21]. Inserting ς_{opt} (Eq. (3)) into Eq. (2) yields:

$$\begin{aligned} \mathcal{F}^\chi(\varrho_\chi) &\leq (\partial_\chi \theta)^2 \left[\frac{4\eta \langle \hat{n} \rangle_{\text{in}} \text{Var}_{\text{in}}(\hat{n})}{(1-\eta) \text{Var}_{\text{in}}(\hat{n}) + \eta \langle \hat{n} \rangle_{\text{in}}} \right] \\ &\quad + (\partial_\chi \eta)^2 \frac{\langle \hat{n} \rangle_{\text{in}}}{\eta(1-\eta)} \\ &\leq \langle \hat{n} \rangle_{\text{in}} \frac{4\eta^2 (\partial_\chi \theta)^2 + (\partial_\chi \eta)^2}{\eta(1-\eta)} =: \mathcal{Q}_\chi. \end{aligned} \quad (4)$$

where the last expression depends only on $\langle \hat{n} \rangle_{\text{in}}$. \mathcal{Q}_χ denotes the maximum information available on χ for any quantum probe and measurement, and therefore the bound we aim to saturate.

Probe states for CPLE — Having found the fundamental limit for CPLE, we next seek an effective strategy for experimentally achieving this bound using single-mode Gaussian

states and homodyne measurements. These were shown to be optimal for lossy-phase estimation in the large photon number limit [34].

Gaussian states are specified by a displacement vector \mathbf{d} comprised of means, $d_i = \langle \hat{x}_i \rangle$, and a matrix Γ comprised of covariances, $\Gamma_{ij} = \frac{1}{2} \langle \hat{x}_i \hat{x}_j + \hat{x}_j \hat{x}_i \rangle - \langle \hat{x}_i \rangle \langle \hat{x}_j \rangle$, of the quadrature operators $\hat{x}_1 = \frac{1}{2}(\hat{a}^\dagger + \hat{a})$ and $\hat{x}_2 = \frac{1}{2}i(\hat{a}^\dagger - \hat{a})$ [35, 36]. Homodyne measurement of a single-mode state provides a measurement of the \hat{x}_1 quadrature [37]. An arbitrary single-mode pure Gaussian state can be defined by the squeezing $\hat{S}(r, \phi) = \exp[\frac{1}{2}r(e^{-i\phi}\hat{a}^2 - e^{i\phi}\hat{a}^{\dagger 2})]$, displacement $\hat{D}(\alpha) = \exp[\alpha(\hat{a}^\dagger - \hat{a})]$, and rotation $\hat{R}(\varphi) = \exp(i\hat{a}^\dagger \hat{a} \varphi)$ operators acting on vacuum: $|\psi^G\rangle = \hat{R}(\varphi)\hat{D}(\alpha)\hat{S}(r, \phi)|0\rangle$ where all arguments are real and the mean number of photons within the state is: $\langle \hat{n} \rangle = \alpha^2 + \sinh^2(r)$. The actions of squeezing, displacement, rotation (phase shift) and loss modify \mathbf{d} and Γ [38]. $|\psi^G\rangle$ will be transformed by Λ_χ to $\tilde{\varrho} = \Lambda_\chi(|\psi^G\rangle)$ with $\tilde{\mathbf{d}} = \mathcal{R}(\varphi + \theta) \begin{pmatrix} \alpha\sqrt{\eta} \\ 0 \end{pmatrix}$ and $\tilde{\Gamma} =$

$$\mathcal{R}(\varphi + \phi/2 + \theta) \frac{1}{4} \begin{pmatrix} \eta e^{-2r} + 1 - \eta & 0 \\ 0 & \eta e^{2r} + 1 - \eta \end{pmatrix} \mathcal{R}^\top(\varphi + \phi/2 + \theta),$$

where $\mathcal{R}(\bullet) = \begin{pmatrix} \cos \bullet & -\sin \bullet \\ \sin \bullet & \cos \bullet \end{pmatrix}$ is the rotation matrix [37].

Throughout the following, tildes over variables refer to properties of the state after Λ_χ has been applied. \mathbf{d} and Γ of $|\psi^G\rangle$ can be observed by setting $\eta=1$ and $\theta=0$ in $\tilde{\mathbf{d}}$ and $\tilde{\Gamma}$.

The QFI of a single-mode Gaussian state $\tilde{\varrho}$ is [39]:

$$\mathcal{F}^\chi(\tilde{\varrho}) = \frac{\text{tr}[(\tilde{\Gamma}^{-1} \partial_\chi \tilde{\Gamma})^2]}{2(1 + \tilde{P}^2)} + \frac{2(\partial_\chi \tilde{P})^2}{1 - \tilde{P}^4} + (\partial_\chi \tilde{\mathbf{d}})^\top \tilde{\Gamma}^{-1} (\partial_\chi \tilde{\mathbf{d}}), \quad (5)$$

where $\tilde{P} = \text{tr}(\tilde{\varrho}^2)$ is the purity. Directly optimising the QFI of a Gaussian state for lossy-phase estimation provides sub-optimal use with homodyne measurement [40]. Because of this, we optimize information related to the parameter dependence on displacement vector $\tilde{\mathbf{d}}$, in the third term of Eq. (5). For lossy-phase estimation it was shown that this information is accessible through homodyne detection and thus we seek to maximise this term by varying the probe $|\psi^G\rangle$.

To do this, the squeezing angle ϕ should be set such that $\partial_\chi \tilde{\mathbf{d}}$ is parallel to the direction of minimum uncertainty in the output state i.e. aligned with the eigenvector of $\tilde{\Gamma}$ with smallest eigenvalue $\tilde{V}_{\text{min}} = [e^{-2r}\eta + (1-\eta)]/4$. A state satisfying this condition is plotted in Fig. 1. In this case, the information contained in displacement vector \mathcal{D} is given by

$$\mathcal{D} := (\partial_\chi \tilde{\mathbf{d}})^\top \tilde{\Gamma}^{-1} (\partial_\chi \tilde{\mathbf{d}}) = \|\partial_\chi \tilde{\mathbf{d}}\|^2 / \tilde{V}_{\text{min}}. \quad (6)$$

The output can be measured using homodyne detection to produce a signal which has a FI of $\mathcal{D} + (\partial_\chi \tilde{V}_{\text{min}})^2 / (2\tilde{V}_{\text{min}}^2)$ [30], which shows that \mathcal{D} is a quantity which can be accessed with a practical measurement. Using an adaptive feedback strategy (e.g. [41]), the squeezing and homodyne angles can be set arbitrarily close to their optimal values. $\partial_\chi \tilde{\mathbf{d}} = (\partial_\chi \theta) \partial_\theta \tilde{\mathbf{d}} + (\partial_\chi \eta) \partial_\eta \tilde{\mathbf{d}}$ where the two terms are always orthogonal, therefore:

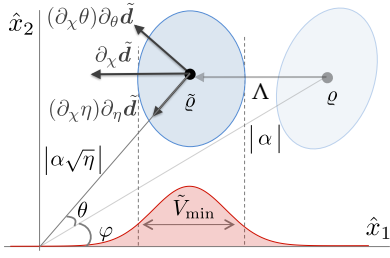


FIG. 1: **Phase-space representation of the transformation of initial state ρ to $\tilde{\rho}$:** after passing through the channel Λ with transmission η and a phase shift of θ . ρ is squeezed in the optimal direction aligned with $\partial_x \tilde{\mathbf{d}}$. The red curve is the homodyne signal when the phase of the local-oscillator is optimized for the measurement.

$$\begin{aligned} \|\partial_x \tilde{\mathbf{d}}\|^2 &= \|(\partial_x \theta) \partial_\theta \tilde{\mathbf{d}}\|^2 + \|(\partial_x \eta) \partial_\eta \tilde{\mathbf{d}}\|^2 \\ &= \alpha^2 [4\eta^2 (\partial_x \theta)^2 + (\partial_x \eta)^2] / 4\eta, \end{aligned}$$

where α is the coherent amplitude of the input state (Fig. 1) and $(\partial_x \theta)^2$ and $(\partial_x \eta)^2$ appear in the same proportions as in \mathcal{Q}_χ (Eq. (4)). It can be observed from Eq. (5) that the QFI achieved with an unsqueezed coherent state as probe is

$$\mathcal{D}|_{r=0} = \langle \hat{n} \rangle_{\text{in}} [4\eta^2 (\partial_x \theta)^2 + (\partial_x \eta)^2] / \eta := \mathcal{S}_\chi, \quad (7)$$

which limits the best precision achievable using classical probes with a single pass through Λ_χ — the standard quantum limit (SQL).

Combining \tilde{V}_{min} and Eq. (6) we find

$$\mathcal{D} = (\langle \hat{n} \rangle_{\text{in}} - n_{\text{sq}}) \frac{4\eta^2 (\partial_x \theta)^2 + (\partial_x \eta)^2}{\eta [e^{-2r} \eta + (1 - \eta)]}. \quad (8)$$

where $\alpha^2 = \langle \hat{n} \rangle_{\text{in}} - n_{\text{sq}}$ has been used and $n_{\text{sq}} = \sinh^2(r)$ is the number of photons contributing to the squeezing of the input state. As $\langle \hat{n} \rangle_{\text{in}}$ grows, $\mathcal{D} / \langle \hat{n} \rangle_{\text{in}}$ will converge to the quantum limit we have found in Eq. (4) i.e. $\lim_{\langle \hat{n} \rangle_{\text{in}} \rightarrow \infty} \mathcal{D} / \langle \hat{n} \rangle_{\text{in}} = \mathcal{Q}_\chi / \langle \hat{n} \rangle_{\text{in}}$ if two conditions are satisfied: First, n_{sq} needs to be a vanishing proportion of the total number of probe photons $\lim_{\langle \hat{n} \rangle_{\text{in}} \rightarrow \infty} n_{\text{sq}} / \langle \hat{n} \rangle_{\text{in}} = 0$. Second, n_{sq} needs to be unbounded with increasing $\langle \hat{n} \rangle_{\text{in}}$, which will ensure e^{-2r} vanishes. In Supplementary Material C [33] we describe a state with finite, and arbitrary, $\langle \hat{n} \rangle_{\text{in}}$ for which $\mathcal{F}^\chi(\rho) = \mathcal{Q}_\chi$, demonstrating \mathcal{Q}_χ is a saturable upper bound (though not of genuine practical utility).

Therefore, we have found that there is no trade-off in the information encoded on a state by the phase and loss of a channel. This is in contrast to the task of estimating phase and loss when there is no correlation [42] which displays a necessary trade-off in the precision to which each parameter could be estimated. Our results also contrast with those reported in Ref. [43], which assume total energy of a probe state including any reference or ancilla (which does not expose the sample) as the resource. With this assumption it was found for the low photon-number regime that there is a trade-off in the sensitivity of the probe state to either loss or phase. Our choice of resource (the total optical power incident on the sample) is

relevant when the sample is delicate. The total optical power in a probe often constitutes a small fraction of the total energy needed for example to generate the quantum probe.

For finite $\langle \hat{n} \rangle_{\text{in}}$, \mathcal{D} can be optimised by choosing the best value of n_{sq} . The optimal amount of squeezing is derived in the Supplementary Material D [33] to be

$$n_{\text{sq}} = \frac{\left(\sqrt{1 - 4(\eta - 1)\eta \langle \hat{n} \rangle_{\text{in}}} - 1 \right)^2}{4(1 - \eta) \left(\sqrt{1 - 4(\eta - 1)\eta \langle \hat{n} \rangle_{\text{in}}} - \eta \right)}, \quad (9)$$

which results in

$$\mathcal{D} = \mathcal{Q}_\chi \frac{2(\eta - 1) \langle \hat{n} \rangle_{\text{in}} + \sqrt{1 - 4(\eta - 1)\eta \langle \hat{n} \rangle_{\text{in}}} - 1}{2(\eta - 1) \langle \hat{n} \rangle_{\text{in}}}.$$

In Fig. 2a the optimal \mathcal{D} for a selection of different values of $\langle \hat{n} \rangle_{\text{in}}$ is plotted over $\eta \in (0, 1)$. The range of $\langle \hat{n} \rangle_{\text{in}} = 10^i$, $i \in \{0, 1, \dots, 8\}$ scale to large numbers but corresponds to low energy e.g. 10^8 photons at $\lambda = 500$ nm equates to 4×10^{-11} J. The plot shows that Gaussian states with modest energies can provide large precision gains for CPLE.

Probe states for DAE — We now turn to DAEs, which refer to measurements of absorption which do not exploit information about any phase imparted by a sample. Previously, a limit on QFI was found for transmission estimation where no phase is imparted by the sample i.e. $\theta = 0$ [17], and Fock states were identified as optimal for this [18]. This bound applies equally for DAE since Fock states are invariant under phase shifts. Since θ is uncorrelated with η and unknown, it cannot increase the QFI associated with η [31], and therefore the limit on QFI for DAE is $\mathcal{Q}|_{\partial_x \theta=0, \partial_x \eta=1} := \mathcal{Q}_\eta$. Similarly $\mathcal{S}_\chi|_{\partial_x \theta=0, \partial_x \eta=1} := \mathcal{S}_\eta$, is the SQL for DAE [18]. However when a Gaussian probe is used, DAE is inequivalent to CPLE with $\partial_x \theta = 0$ since the probe state will be transformed by any phase shift present. For instance, the strategy for CPLE described above using Gaussian states does not work for DAE as the correct homodyne measurement setting depends on the phase imparted by the sample — we therefore seek an alternative strategy.

Intensity measurements are unaffected by the phase of the detected light, and therefore provide a way to decouple the effects of sample absorption and any phase shift. To find useful strategies for DAE, we consider the statistical information \mathcal{N} contained measurement of the mean intensity which will be detected $\langle \hat{n} \rangle_{\text{out}} = \eta \langle \hat{n} \rangle_{\text{in}}$, which can be found most simply using standard error propagation:

$$\begin{aligned} \mathcal{N} &:= 1 / \text{Var}(\eta) = (\partial_\eta \langle \hat{n} \rangle_{\text{out}})^2 / \text{Var}_{\text{out}}(\hat{n}) \\ &= (\langle \hat{n} \rangle_{\text{in}})^2 / [\eta^2 \text{Var}_{\text{in}}(\hat{n}) + \eta(1 - \eta) \langle \hat{n} \rangle_{\text{in}}], \end{aligned} \quad (10)$$

which applies for arbitrary states. Considering only the mean intensity ensures complex measurement and estimation procedures are not needed and \mathcal{N} plays a role analogous to FI.

Loss reduces the amplitude of a Gaussian state, and so a natural probe state to consider for DAE is an amplitude-squeezed Gaussian state, $|\psi^G\rangle|_{\phi=0}$. Note that for this state

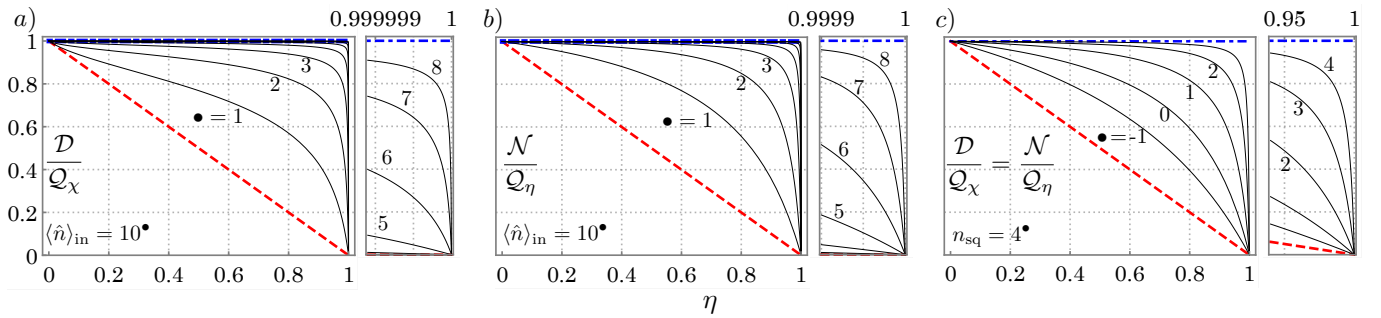


FIG. 2: **Comparing strategies for CPLE and DAE with their respective quantum limits:** Within each plot the red dashed line shows the SQL and all plots are normalised to the quantum limit \mathcal{Q}_χ or \mathcal{Q}_η . Plots a) and b) display the amount of statistical information \mathcal{D} and \mathcal{N} encoded onto the displacement vector (mean number of photons) of a squeezed coherent state for CPLE and DAE respectively. The inset shows that even for very low absorption these states approach the quantum limit for modest energies. Statistical information plotted for varying input mean photon number operating with the optimal squeezing value presented in a) Eq. (9) and b) Supplementary Material E [33]. c) Amount of statistical information \mathcal{D} (\mathcal{N}) encoded onto the displacement vector of a squeezed coherent state for CPLE (DAE) when α is large. We note that for a)-c), inset figures display the same y-axis scale as the main plots, whilst having an x-axis scale as labelled at the top of the plot.

$\text{Var}_{\text{in}}(\hat{n}) = 2 \text{tr}^2 \Gamma - \frac{3}{4} + (\langle \hat{n} \rangle_{\text{in}} - n_{\text{sq}}) e^{-2r}$ [44] and $\text{tr}^2 \Gamma = \mathcal{O}(n_{\text{sq}}^2)$. Asymptotic optimality $\lim_{\langle \hat{n} \rangle_{\text{in}} \rightarrow \infty} \mathcal{N}/\langle \hat{n} \rangle_{\text{in}} = \mathcal{Q}_\eta/\langle \hat{n} \rangle_{\text{in}}$ can be achieved if n_{sq} is unbounded (to ensure e^{-2r} vanishes) and also a vanishing proportion of $\sqrt{\langle \hat{n} \rangle_{\text{in}}}$. This ensures that the photon number variance of the input state contributes negligibly to the denominator of expression on the second line of Eq. (10). Also shown in Eq. (10) is that in order to maximize \mathcal{N} , the photon number variance of the input should be minimised for a given $\langle \hat{n} \rangle_{\text{in}}$ independently of η . In Fig. 2b the optimal \mathcal{N} for different values of $\langle \hat{n} \rangle_{\text{in}}$ is plotted over $\eta \in (0, 1)$. (see Supplementary Material E [33] for the optimization). This plot shows that Gaussian states with modest energies can provide large precision gains for DAE.

Multi-pass strategies — Rather than using non-classical states, it is sometimes possible to increase precision beyond the SQL by sending a classical (coherent state) optical probe through the sample multiple times [34] or by optimising experimental parameters [45]. Recently it was shown that, for lossy-phase estimation, multi-pass strategies could obtain 60% of the quantum limit on FI for a given number of photons incident upon the sample over all passes and for any values of the phase shift and loss. In Supplementary Material F [33] we extend this result and show that multi-pass strategies provide exactly the same benefits for CPLE and DAE as they do for lossy-phase estimation. This exact correspondence holds even when lossy components are used to perform the multi-pass strategy.

Practical application — At present the highest amount of optical squeezing measured is 15 dB [46] ($n_{\text{sq}} = 7.4$). By explicitly considering large α we can quantify the quantum advantage, Δ , squeezing brings to both CPLE and DAE:

$$\Delta = \lim_{\alpha \rightarrow \infty} \mathcal{N}/\mathcal{S}_\eta = \lim_{\alpha \rightarrow \infty} \mathcal{D}/\mathcal{S}_\chi = \frac{1}{e^{-2r\eta} + (1 - \eta)}, \quad (11)$$

observing that the enhancement provided for both DAE and CPLE is the same and for a fixed sample transmission η depends only on the input squeezing parameter r . The precision

gains which squeezing brings to probe states with large α is plotted in Fig. 2.c.

For CPLE, Eq. (11) encouragingly indicates that a small amount of squeezing can substantially increase the precision of a measurement. Generating and detecting Fock states is a non-trivial task and as such only low photon number Fock states have been generated [47, 48]; these states may prove useful for the measurement of samples which are damaged by very few photons. The Gaussian probe state we have studied can be created by the displacement of a squeezed vacuum state to contain much larger amounts of power [49], benefiting absorption measurements far beyond the few photon regime.

We highlight Ref. [6] which reported absorption measurements with 10 μW of incident laser light (10^{13} photons per second) at 633 nm to detect the presence of single molecules. Using a balanced photodetector the effective intensity fluctuations in the laser light were reduced to the shot-noise limit. Using Eq. (11) and taking η to be 0.95, 15 dB of squeezing [50] in this experiment would reduce the contribution to the mean-squared error (MSE) from fundamental fluctuations by a factor of 12.5. This is 79% of the advantage provided by using 10^{13} photons per second in ideal Fock states. This would allow an increase in precision whilst maintaining incident optical power, for example at a level just below the photobleaching threshold. Strategies using squeezed light in general can offer improvements due to other limitations. Examples include Refs. [51, 52] which introduce a squeezed light source to tackle the competing interferometric noise contributions from shot and back-action noise in gravitational wave astronomy.

As well as reducing the MSE, an alternative benefit for this quantum strategy is that the same precision can be achieved with a factor of 12.5 reduction in input intensity. This can provide an opportunity to increase the frame rate of the sensor, allowing faster dynamics to be observed [53]. In general, squeezing strategies should target systems that are shot-noise limited [54] and seek an increase in precision in the range that

quantum states of light can provide [55].

Conclusion — Our results further indicate that for estimating parameters of linear optical transformations with non-unit transmissivity, the information encoded in the coarse-grained properties of a state, such as the mean intensity or mean quadrature value, is very close to the fundamental limit on the information encoded on an entire state [14, 34]. We anticipate the quantum limit on CPLE and our Gaussian state strategy can be generalized to multiparameter estimation problems [56] and perhaps even to precision estimation of general-linear mode transformations.

Acknowledgments — We thank J.P. Dowling and D.H. Mahler for helpful discussions. This work was supported by EPSRC, ERC, PICQUE, BBOI, US Army Research Office (ARO) Grant No. W911NF-14-1-0133, U.S. Air Force Office of Scientific Research (AFOSR) and the Centre for Nanoscience and Quantum Information (NSQI). E.J.A. was supported by the Quantum Engineering Centre for Doctoral Training, EPSRC grant EP/L015730/1 and EPSRC Doctoral Prize Fellowship EP/R513179/1. J.L.O.B. acknowledges a Royal Society Wolfson Merit Award and a Royal Academy of Engineering Chair in Emerging Technologies. J.C.F.M. and J.L.O'B acknowledge fellowship support from EPSRC. J.C.F.M. acknowledges support from ERC starting grant ERC-2018-STG803665. T.M.S. was supported by the Benjamin-Meaker visiting fellowship and the ARC Centre of Excellence in Engineered Quantum Systems (EQUS, CE170100009).

* Electronic address: euan.allen@bristol.ac.uk

- [1] V. Giovannetti, S. Lloyd, and L. Maccone, “Quantum-enhanced measurements: beating the standard quantum limit,” *Science*, vol. 306, no. 5700, pp. 1330–1336, 2004.
- [2] T. M. Stace, “Quantum limits of thermometry,” *Physical Review A*, vol. 82, no. 1, p. 011611, 2010.
- [3] G.-W. Truong, J. Anstie, E. May, T. Stace, and A. Luiten, “Accurate lineshape spectroscopy and the boltzmann constant,” *Nature communications*, vol. 6, p. 8345, 2015.
- [4] M. A. Taylor and W. P. Bowen, “Quantum metrology and its application in biology,” *Phys. Rep.*, vol. 615, pp. 1–59, 2016.
- [5] J. Aasi, J. Abadie, B. P. Abbott, R. Abbott, T. D. Abbott, M. R. Abernathy, C. Adams, T. Adams, P. Addesso, R. X. Adhikari, *et al.*, “Enhanced sensitivity of the ligo gravitational wave detector by using squeezed states of light,” *Nature Photon.*, vol. 7, no. 8, pp. 613–619, 2013.
- [6] P. Kukura, M. Celebrano, A. Renn, and V. Sandoghdar, “Single-molecule sensitivity in optical absorption at room temperature,” *J. Phys. Chem. Lett.*, vol. 1, no. 23, pp. 3323–3327, 2010.
- [7] C. M. Caves, “Quantum-mechanical noise in an interferometer,” *Phys. Rev. D.*, vol. 23, no. 8, p. 1693, 1981.
- [8] U. Dorner, R. Demkowicz-Dobrzanski, B. J. Smith, J. S. Lundeen, W. Wasilewski, K. Banaszek, and I. A. Walmsley, “Optimal quantum phase estimation,” *Phys. Rev. Lett.*, vol. 102, no. 4, p. 040403, 2009.
- [9] R. Demkowicz-Dobrzanski, U. Dorner, B. J. Smith, J. S. Lundeen, W. Wasilewski, K. Banaszek, and I. A. Walmsley, “Quantum phase estimation with lossy interferometers,” *Phys. Rev. A*, vol. 80, no. 1, p. 013825, 2009.
- [10] M. Kacprowicz, R. Demkowicz-Dobrzanski, W. Wasilewski, K. Banaszek, and I. A. Walmsley, “Experimental quantum-enhanced estimation of a lossy phase shift,” *Nature Photon.*, vol. 4, no. 6, pp. 357–360, 2010.
- [11] N. Thomas-Peter, B. J. Smith, A. Datta, L. Zhang, U. Dorner, and I. A. Walmsley, “Real-world quantum sensors: evaluating resources for precision measurement,” *Phys. Rev. Lett.*, vol. 107, no. 11, p. 113603, 2011.
- [12] H. Cable and G. A. Durkin, “Parameter estimation with entangled photons produced by parametric down-conversion,” *Phys. Rev. Lett.*, vol. 105, no. 1, p. 013603, 2010.
- [13] B. M. Escher, R. L. de Matos Filho, and L. Davidovich, “General framework for estimating the ultimate precision limit in noisy quantum-enhanced metrology,” *Nature Phys.*, vol. 7, no. 5, pp. 406–411, 2011.
- [14] R. Demkowicz-Dobrzanski, K. Banaszek, and R. Schnabel, “Fundamental quantum interferometry bound for the squeezed-light-enhanced gravitational wave detector GEO 600,” *Phys. Rev. A*, vol. 88, no. 4, p. 041802, 2013.
- [15] B. Yurke and E. A. Whittaker, “Squeezed-state-enhanced frequency-modulation spectroscopy,” *Opt. Lett.*, vol. 12, no. 4, pp. 236–238, 1987.
- [16] E. S. Polzik, J. Carri, and H. J. Kimble, “Spectroscopy with squeezed light,” *Phys. Rev. Lett.*, vol. 68, no. 20, p. 3020, 1992.
- [17] A. Monras and M. G. A. Paris, “Optimal quantum estimation of loss in bosonic channels,” *Phys. Rev. Lett.*, vol. 98, no. 16, p. 160401, 2007.
- [18] G. Adesso, F. Dell’Anno, S. De Siena, F. Illuminati, and L. A. M. Souza, “Optimal estimation of losses at the ultimate quantum limit with non-gaussian states,” *Phys. Rev. A*, vol. 79, no. 4, p. 040305, 2009.
- [19] G. Brida, M. Genovese, and I. R. Berchera, “Experimental realization of sub-shot-noise quantum imaging,” *Nature Photon.*, vol. 4, no. 4, pp. 227–230, 2010.
- [20] J. Sabines-Chesterking, R. Whittaker, S. Joshi, P. Birchall, P. Moreau, A. McMillan, H. Cable, J. O’Brien, J. Rarity, and J. Matthews, “Sub-shot-noise transmission measurement enabled by active feed-forward of heralded single photons,” *Physical Review Applied*, vol. 8, no. 1, p. 014016, 2017.
- [21] P.-A. Moreau, J. Sabines-Chesterking, R. Whittaker, S. K. Joshi, P. M. Birchall, A. McMillan, J. G. Rarity, and J. C. Matthews, “Demonstrating an absolute quantum advantage in direct absorption measurement,” *Scientific reports*, vol. 7, no. 1, p. 6256, 2017.
- [22] N. Liu and H. Cable, “Quantum-enhanced multi-parameter estimation for unitary photonic systems,” *Quantum Science and Technology*, vol. 2, no. 2, p. 025008, 2017.
- [23] M. Gessner, L. Pezzè, and A. Smerzi, “Sensitivity bounds for multiparameter quantum metrology,” *Physical review letters*, vol. 121, no. 13, p. 130503, 2018.
- [24] T. J. Proctor, P. A. Knott, and J. A. Dunningham, “Multiparameter estimation in networked quantum sensors,” *Physical review letters*, vol. 120, no. 8, p. 080501, 2018.
- [25] M. Szczykulska, T. Baumgratz, and A. Datta, “Multi-parameter quantum metrology,” *Advances in Physics: X*, vol. 1, no. 4, pp. 621–639, 2016.
- [26] S. Ragy, M. Jarzyna, and R. Demkowicz-Dobrzanski, “Compatibility in multiparameter quantum metrology,” *Physical Review A*, vol. 94, no. 5, p. 052108, 2016.
- [27] R. Nichols, P. Liuzzo-Scorpo, P. A. Knott, and G. Adesso, “Multiparameter gaussian quantum metrology,” *Physical Review A*, vol. 98, no. 1, p. 012114, 2018.

- [28] K. Libbrecht and M. Libbrecht, “Interferometric measurement of the resonant absorption and refractive index in rubidium gas,” *American journal of physics*, vol. 74, no. 12, pp. 1055–1060, 2006.
- [29] U. L. Andersen, T. Gehring, C. Marquardt, and G. Leuchs, “30 years of squeezed light generation,” *Physica Scripta*, vol. 91, no. 5, p. 053001, 2016.
- [30] A. W. Van der Vaart, *Asymptotic statistics*, vol. 3. Cambridge university press, 2000.
- [31] C. W. Helstrom, *Quantum detection and estimation theory*. Academic press, 1976.
- [32] S. L. Braunstein and C. M. Caves, “Statistical distance and the geometry of quantum states,” *Phys. Rev. Lett.*, vol. 72, no. 22, p. 3439, 1994.
- [33] See Supplementary Material for a) proof of the unitary dilation, b) derivation of Eq. (1), c) proof of the saturation of Q_x , d) derivation of the optimal squeezing value presented in Eq. 8, e) details of the optimisation of the parameter \mathcal{N} , f) for details on multipass strategies for CPLE.
- [34] P. M. Birchall, J. L. O’Brien, J. C. Matthews, and H. Cable, “Quantum-classical boundary for precision optical phase estimation,” *Physical Review A*, vol. 96, no. 6, p. 062109, 2017.
- [35] R. Simon, E. C. G. Sudarshan, and N. Mukunda, “Gaussian-wigner distributions in quantum mechanics and optics,” *Phys. Rev. A*, vol. 36, no. 8, p. 3868, 1987.
- [36] R. Simon, N. Mukunda, and B. Dutta, “Quantum-noise matrix for multimode systems: U (n) invariance, squeezing, and normal forms,” *Phys. Rev. A*, vol. 49, no. 3, p. 1567, 1994.
- [37] R. Loudon and P. L. Knight, “Squeezed light,” *J. Mod. Opt.*, vol. 34, no. 6-7, pp. 709–759, 1987.
- [38] C. Weedbrook, S. Pirandola, R. García-Patrón, N. J. Cerf, T. C. Ralph, J. H. Shapiro, and S. Lloyd, “Gaussian quantum information,” *Reviews of Modern Physics*, vol. 84, no. 2, p. 621, 2012.
- [39] O. Pinel, P. Jian, N. Treps, C. Fabre, and D. Braun, “Quantum parameter estimation using general single-mode gaussian states,” *Phys. Rev. A*, vol. 88, no. 4, p. 040102, 2013.
- [40] M. Aspachs, J. Calsamiglia, R. Muñoz-Tapia, and E. Bagan, “Phase estimation for thermal gaussian states,” *Phys. Rev. A*, vol. 79, no. 3, p. 033834, 2009.
- [41] A. A. Berni, T. Gehring, B. M. Nielsen, V. Händchen, M. G. Paris, and U. L. Andersen, “Ab initio quantum-enhanced optical phase estimation using real-time feedback control,” *Nature Photonics*, vol. 9, no. 9, p. 577, 2015.
- [42] P. J. D. Crowley, A. Datta, M. Barbieri, and I. A. Walmsley, “Tradeoff in simultaneous quantum-limited phase and loss estimation in interferometry,” *Phys. Rev. A*, vol. 89, no. 2, p. 023845, 2014.
- [43] H. T. Dinani, M. K. Gupta, J. P. Dowling, and D. W. Berry, “Quantum-enhanced spectroscopy with entangled multiphoton states,” *Phys. Rev. A*, vol. 93, no. 6, p. 063804, 2016.
- [44] V. Dodonov, O. Man’ko, and V. Man’ko, “Photon distribution for one-mode mixed light with a generic gaussian wigner function,” *Phys. Rev. A*, vol. 49, no. 4, p. 2993, 1994.
- [45] E. J. Allen, J. Sabines-Chesterking, A. McMillan, S. K. Joshi, P. S. Turner, and J. C. Matthews, “Quantum absorbance estimation and the beer-lambert law,” *arXiv preprint arXiv:1912.05870*, 2019.
- [46] H. Vahlbruch, M. Mehmet, K. Danzmann, and R. Schnabel, “Detection of 15 db squeezed states of light and their application for the absolute calibration of photoelectric quantum efficiency,” *Phys. Rev. Lett.*, vol. 117, no. 11, p. 110801, 2016.
- [47] M. Cooper, L. J. Wright, C. Söller, and B. J. Smith, “Experimental generation of multi-photon fock states,” *Opt. Express.*, vol. 21, no. 5, pp. 5309–5317, 2013.
- [48] K. R. Motes, R. L. Mann, J. P. Olson, N. M. Studer, E. A. Bergeron, A. Gilchrist, J. P. Dowling, D. W. Berry, and P. P. Rohde, “Efficient recycling strategies for preparing large fock states from single-photon sources: Applications to quantum metrology,” *Physical Review A*, vol. 94, no. 1, p. 012344, 2016.
- [49] K. Schneider, R. Bruckmeier, H. Hansen, S. Schiller, and J. Mlynek, “Bright squeezed-light generation by a continuous-wave semimonolithic parametric amplifier,” *Opt. Lett.*, vol. 21, no. 17, pp. 1396–1398, 1996.
- [50] This level of measured squeezing, reported in in [46], is the current experimental record. This value shows what is possible, despite experimental practicalities such as detector efficiency and mode overlap. . In [46], the total experimental efficiency achieved was 97.5%. Conversion to decibels from the squeezing parameter r in Eq. (11) can be performed using $dB = 10 \log_{10}(e^{-2r})$.
- [51] F. Acernese, M. Agathos, L. Aiello, A. Allocca, A. Amato, S. Ansoldi, S. Antier, M. Arène, N. Arnaud, S. Ascenzi, *et al.*, “Increasing the astrophysical reach of the advanced virgo detector via the application of squeezed vacuum states of light,” *Physical Review Letters*, vol. 123, no. 23, p. 231108, 2019.
- [52] M. Tse, H. Yu, N. Kijbunchoo, A. Fernandez-Galiana, P. Dupej, L. Barsotti, C. Blair, D. Brown, S. Dwyer, A. Effler, *et al.*, “Quantum-enhanced advanced ligo detectors in the era of gravitational-wave astronomy,” *Physical Review Letters*, vol. 123, no. 23, p. 231107, 2019.
- [53] M. A. Taylor, J. Janousek, V. Daria, J. Knittel, B. Hage, H.-A. Bachor, and W. P. Bowen, “Biological measurement beyond the quantum limit,” *Nature Photonics*, vol. 7, no. 3, p. 229, 2013.
- [54] D. Hillmann, H. Spahr, C. Hain, H. Sudkamp, G. Franke, C. Pfäffle, C. Winter, and G. Hüttmann, “Aberration-free volumetric high-speed imaging of in vivo retina,” *Scientific reports*, vol. 6, p. 35209, 2016.
- [55] N. Nassif, B. Cense, B. H. Park, S. H. Yun, T. C. Chen, B. E. Bouma, G. J. Tearney, and J. F. de Boer, “In vivo human retinal imaging by ultrahigh-speed spectral domain optical coherence tomography,” *Optics letters*, vol. 29, no. 5, pp. 480–482, 2004.
- [56] F. Albarelli, J. F. Friel, and A. Datta, “Evaluating the holevo cramer-rao bound for multi-parameter quantum metrology,” *arXiv preprint arXiv:1906.05724*, 2019.